High-pressure layered structure of carbon disulfide

S. Shahab Naghavi,[1,2,3] Yanier Crespo,[4,5] Roman Martoňák,[6] and Erio Tosatti[1,2,4]

[1]*International School for Advanced Studies, Via Bonomea 265, I-34136 Trieste, Italy*
[2]*CNR-IOM Democritos National Simulation Center, Via Bonomea 265, I-34136 Trieste, Italy*
[3]*Department of Materials Science and Engineering, Northwestern University, Evanston, Illinois 60208, USA*
[4]*International Centre for Theoretical Physics, Strada Costiera 11, I-34151 Trieste, Italy*
[5]*International Institute of Physics, Avenida Odilon Gomes de Lima, 1722, Capim Macio, CEP 59078-400, Natal RN, Brazil*
[6]*Department of Experimental Physics, Comenius University in Bratislava, Mlynská Dolina F2, 842 48 Bratislava, Slovakia*

Solid CS_2 is superficially similar to CO_2, with the same *Cmca* molecular crystal structure at low pressures, which has suggested similar phases also at high pressures. We carried out an extensive first-principles evolutionary search in order to identify the zero-temperature lowest-enthalpy structures of CS_2 for increasing pressure up to 200 GPa. Surprisingly, the molecular *Cmca* phase does not evolve into β-cristobalite as in CO_2 but transforms instead into phases HP2 and HP1, both recently described in high-pressure SiS_2. HP1 in particular, with a wide stability range, is a layered $P2_1/c$ structure characterized by pairs of edge-sharing tetrahedra and is theoretically more robust than all other CS_2 phases discussed so far. Its predicted Raman spectrum and pair correlation function agree with experiment better than those of β-cristobalite, and further differences are predicted between their respective IR spectra. The band gap of HP1-CS_2 is calculated to close under pressure, yielding an insulator-metal transition near 50 GPa, in agreement with experimental observations. However, the metallic density of states remains modest above this pressure, suggesting a different origin for the reported superconductivity.

PACS number(s): 61.50.Ks, 71.30.+h, 74.10.+v

I. INTRODUCTION

The crystal structure of even extremely stable molecular carbon compounds like CO_2 is known to transform radically at high pressures where, above ~ 50 GPa, the carbon coordination is found, both experimentally [1] and theoretically [2], to switch from two in the molecular structure *Cmca* to four in the β-cristobalite structure [3,4]. Similar pressure-induced structural transformations can reasonably be expected to occur in a compound such as CS_2, which is the focus of the present study and which presents obvious similarities to CO_2. Indeed, CS_2 adopts at zero pressure the same *Cmca* molecular crystal structure as metastable phase III of CO_2 at moderate pressures between 15 and 50 GPa. However, the binding in CS_2 is much weaker than in CO_2, with a smaller electronic band gap and a positive formation enthalpy of about 88.7 kJ/mol as opposed to a large negative one of -393.509 kJ/mol for CO_2 [5,6]. Thermodynamically, that makes decomposition and phase separation into elementary carbon and sulfur a thermodynamic necessity for CS_2 at equilibrium already at ambient pressure and presumably even more so at higher pressures. In spite of that intrinsic thermodynamical metastability, solid CS_2 phases do exist, clearly for kinetic reasons, and are reported at ambient pressure not to decompose in measurable times, at least below ≈ 560 K [7,8], a temperature rising even further at high pressures, possibly up to 1000 K at 70 GPa [7]. At high pressures but low temperatures, x-ray data have shown evidence of structural transitions of CS_2 from the molecular phase to polymeric phases with C-S coordinations rising from two (*Cmca*) to three (CS3) to four (CS4) [7] and higher. With the exception of the CS3 phase near 20 GPa, the high-pressure structural behavior has been postulated to be similar to that of CO_2, implying (not unreasonably) that CS4 could be β-cristobalite. In CS_2 a detailed interpretation of high-pressure experimental data is further complicated by a large amount of structural disorder, particularly in the CS4

phase where only broad, rather than sharp, Bragg peaks are present in the diffraction pattern [7]. With that rationalization of the fourfold coordinated state of CS_2 near 50 GPa through simple analogy with CO_2, density functional theory (DFT) studies have considered β-cristobalite ($I\bar{4}2d$, also referred to as chalcopyrite) and tridymite ($P2_12_12_1$) for comparison with experimental data. Because of the lack of sharp diffraction peaks or other distinctive features, that comparison nevertheless appears somewhat elusive. The tridymite structure shows slightly better agreement with experiment but represents a thermodynamically less likely candidate than β-cristobalite since its calculated DFT enthalpy is 0.3–0.4 eV/molecule higher [7]. The electronic structure of either fourfold coordinated crystal structure agrees with the observed metallization in the region from 40 GPa upwards [7,9]. Besides that, in more recent experiments performed on the high-pressure metallic phases of CS_2, resistivity showed evidence of superconductivity at 4–6 K over a broad pressure range from 50 to 172 GPa [9].

From the theoretical point of view it is, of course, inadequate to merely trust the analogy between CS_2 and CO_2 and extend it even to very high pressures. To expand somewhat our view we instead consider that CO_2 and CS_2 are members of a broader family of IV–VI AB_2 compounds, including SiO_2, silica, and SiS_2, none of which is molecular at zero pressure. Silica is very well known for a number of tetrahedrally coordinated polymorphs, including α- and β-quartz, α- and β-cristobalite, α- and β-tridymite, coesite, etc. Much less studied until recently, SiS_2 exhibits totally different phases starting off at zero pressure with an orthorhombic (so-called NP) crystal structure made up of edge-sharing carbon-centered tetrahedra (see Ref. [10]) Very recently, the high-pressure phases of SiS_2 were experimentally characterized [10], and a whole sequence of phases (HP1, HP2, HP3) was described in which the tetrahedra did not disappear but simply changed their mutual connectivity.
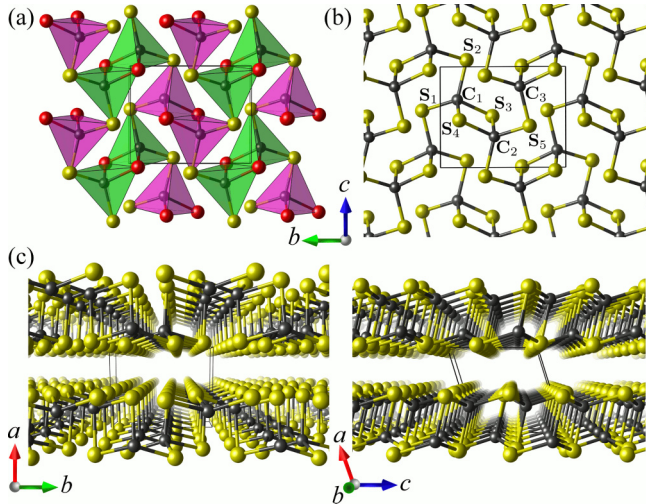
FIG. 1. (Color online) The $P2_1/c$ layered crystal structure, named HP1 after that reported for SiS_2 [10], viewed along the a, b, and c axes. Each layer is made up of two pairs of CS_4 tetrahedra. The two tetrahedra in each pair are joined by the edge, with S edge atoms shown in red. At ≈ 50 GPa the interlayer distance is about 2.1 Å. Full structural data are given in Table I.

Based on the limited available high-pressure data, solid CS_2 is, at the moment, the least understood member of this highly important class of solids. Even if it starts at zero pressure with the same molecular *Cmca* structure that CO_2 adopts at moderate pressure, CS_2 does not necessarily develop at very high pressures the same structures as CO_2. To fill this remaining knowledge gap we conducted an unbiased theoretical crystal structure search to explore high-pressure structures of CS_2. This search revealed that at high pressures where the carbon coordination is four the β-cristobalite structural motif is indeed superseded by a novel, robust, and unsuspected layered network of tetrahedra. Recently, fresh high-pressure experimental work on SiS_2 appeared [10] that reported the very same structure, designated there as HP1. Our theoretical search now finds the tetrahedra-based structure of CS_2, which is lowest in enthalpy over a wide range of pressures from 30 to 170 GPa, to be structurally identical to the HP1 structure of SiS_2 [10] (see Fig. 1). Based on this HP1 structure of CS_2 we calculated the Raman spectra and pair distribution functions and found it to agree better with experimental data than those of β-cristobalite, the high-pressure structure of CO_2. We also obtained predictions for the infrared absorption spectra not yet available experimentally that will hopefully serve in the future to experimentally corroborate or discard our predictions. The calculated electronic structure of high-pressure metallized HP1-CS_2 moreover indicates a small Fermi level density of states, calling into question the intrinsic nature of the observed superconductivity.

This paper is organized as follows. In Sec. II we present the details of our structural search and subsequent analysis. In Sec. III we present the structural results of our search. In Secs. IV and V we analyze the lattice dynamics, Raman spectra, and electronic structure of the new phase. In Sec. VI we summarize the results and draw conclusions.

II. COMPUTATIONAL METHODS

The search for low-enthalpy structures of CS_2 was carried out by exploiting an evolutionary algorithm (EA), as implemented in the USPEX code [11–15]. The EA was run in conjunction with *ab initio* electronic structure calculations and relaxations based on standard DFT. The Perdew-Burke-Ernzerhof (PBE) [16] generalized gradient approximation (GGA) as implemented in VASP (Vienna Ab initio Simulation Package) [17] employed the projector augmented-plane-wave (PAW) method [18,19]. The energy cutoff for the plane-wave basis was set to 550 eV to ensure full convergence. The Brillouin zone was sampled by Monkhorst-Pack meshes with a resolution of $2\pi \times 0.05\,\text{Å}^{-1}$. Since at low pressures the dispersion forces are important, we employed the optB86b-vdW scheme [20,21] based on the van der Waals density functional [22] for enthalpy calculations. Lattice zero-point energies were not included, and temperature was assumed to be zero throughout. The phonon, Raman, and IR spectra were instead calculated in linear response as implemented in the QUANTUM ESPRESSO suite of programs within the local-density approximation (LDA) [23]. For that, the GGA input structures were further relaxed with LDA before carrying out the phonon calculations.

Brute-force application of the EA structural search algorithm to a compound such as CS_2 with a positive formation enthalpy should lead by necessity to chemical decomposition and outright disappearance of the compound itself. As stated above, even at ambient pressure molecular CS_2 is metastable, meaning it is locally stable mechanically, and temporarily survives due to exceedingly slow kinetics, while it is intrinsically unstable on thermodynamic grounds. The EA search ignores kinetics and will therefore lead to decomposition, given a large enough supercell. In this study, where we wish to find and study the high-pressure metastable phases of the undecomposed compound, a strict CS_2 stoichiometry was assumed with an EA cell chosen to contain 12 atoms, i.e., four CS_2 molecular units. Even if it is small, that cell is actually still large enough to show decomposition and phase separation into carbon and sulfur in an unrestricted EA search. We therefore artificially prevented decomposition by constraining the EA search to avoid the formation of C-C and S-S first-neighbor bonds. This allows us to find the high-pressure crystal structures where decomposition, total or partial, is artificially suppressed. It should be noted that while the artificial nature of this constraint is such that it may endanger the formation of some denser structures at higher pressures, various octahedral structures were still created, but their calculated enthalpies were considerably higher with respect to the tetrahedral ones. With this constraint, the crystal structure search was performed at 0, 26, 38, 75, 120, and 170 GPa. The EA initial population (the number of structures in the starting generation) was set to 120, a large number chosen in order to densely sample the configuration space of the random search; the population was later reduced to 30 in the following generations.

III. CRYSTAL STRUCTURES, PAIR CORRELATIONS, AND X-RAY DIFFRACTION SPECTRA

The EA search produced a large variety of structures. In particular, near $P = 0$ we reproduced the known molecular
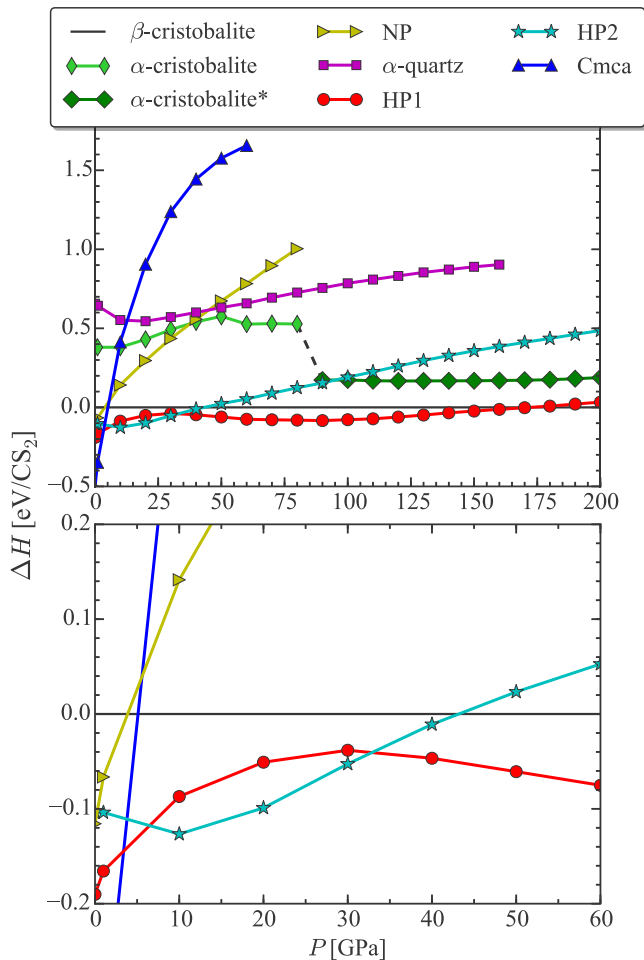
FIG. 2. (Color online) Zero-temperature enthalpy for some optimized structures of CS_2, plotted relative to β-cristobalite ($I\bar{4}2d$). No structures with carbon coordinations of three or larger than four are considered. Structures HP1 ($P2_1/c$), HP2 ($P2_1/c$), and NP (*Ibam*) are based on CS_4 tetrahedra. The relative stability of HP2 between 10 and 30 GPa is marginal and possibly unreliable. α-cristobalite* ($P2_12_12_1$, no. 19) is a high-pressure version of regular α-cristobalite ($P4_12_12$, no. 92) in which symmetry is reduced through a rotation of the tetrahedral environment of the carbon atom.

Cmca structure, validating the scheme. Since, experimentally, the CS_4 tetrahedral structure was created at 30 GPa [9], we further focused on the search for tetrahedral structures at pressures above 26 GPa. In Fig. 2 we present the low-enthalpy phases found by EA - *Cmca* for the molecular structure and α- and β-cristobalite as well as HP1 for nonmolecular tetrahedra-based phases. To complete the comparison, we also added in the well-known α-quartz structure from SiO_2. As explained above, although all these structures are metastable against decomposition, those which we describe are at least mechanically stable under structural optimization and dynamically stable as shown by phonon calculations (see, e.g., Fig. 5), thus representing local enthalpy minima. At any given pressure these phases compete, so they are all doubly metastable except for that with the lowest enthalpy. It makes sense to consider them all anyway because that broader picture clarifies the

relative stability margins and also because metastable phases commonly appear experimentally for kinetic reasons.

Except for 0 GPa, where molecular *Cmca* was found to prevail, in agreement with experiment, the most important structure obtained by the EA search at high pressures was $P2_1/c$ (HP1). This monoclinic layered structure is quite interesting. We optimized this structure at 50 GPa and found its enthalpy to be 1.48 eV/molecule above that of full decomposition to diamond and SIII sulphur (for comparison, the formation enthalpy of CS_2 at normal conditions is 0.92 eV/molecule so pressure indeed tends to favor decomposition). The structural parameters obtained at this pressure are listed in Table I. As shown in Fig. 1, the carbon coordination is four but is quite different from that of β-cristobalite. Each layer consists of four CS_4 tetrahedra, or, more accurately, two pairs of tetrahedra. Tetrahedra of different pairs (different colors in Fig. 1) share a corner sulfur, but two tetrahedra in the same pair (same color) share an edge made up of two sulfurs. As simple as it looks, this structure was at first a total surprise: we designated it "shahabite" because of the lack of an existing name. We found subsequently that the very same structure was very recently [10] observed and called HP1 in the phase diagram of SiS_2 at the much lower pressure of 2.8 GPa (actually, it had apparently been observed in SiS_2 a long time ago [24] but was not resolved).

In Ref. [10] another monoclinic phase with space group $P2_1/c$ denoted as HP2 was observed to follow HP1 at a pressure of 3.5 GPa in SiS_2. Unlike HP1, which is layered and involves four CS_2 units, the HP2 phase consists of 12 CS_2 units, arranged in a three-dimensional covalent network. For the sake of completeness we calculated enthalpies in CS_2 for optimized HP2 and for the chainlike orthorhombic phase with space group *Ibam* which was denoted in Ref. [10] as NP, the structure of SiS_2 at ambient pressure. The structural parameters of these theoretical CS_2 phases (HP1, HP2, and NP) at various relevant pressures are listed in Table I. We do not study here the tridymite phase considered by Ref. [7]. We have not found it in our EA search and moreover we found it to be unstable at 50 GPa, spontaneously converting into a low-symmetry structure.

The relative enthalpies calculated for these structures are shown in Fig. 2. The *Cmca* molecular phase prevailing at low pressures is quickly supplanted by $I\bar{4}2d$ β-cristobalite at about $\approx$10 GPa. At the same time, however, the $P2_1/c$ tetrahedra-based structures appear, preempting this transformation and replacing the *Cmca* molecular structure already at about 5 GPa. Upon increasing pressure, the two structures (HP1 and HP2) remain nearly isoenthalpic up to 30 GPa. Above that pressure the HP1 layered structure clearly prevails; its enthalpy remains lower than that of β-cristobalite by a substantial amount, exceeding the estimated computational errors of about 10 meV/molecular unit, up to 160 GPa. The same HP1 structure which we found here appears in SiS_2 at much lower pressures than in CS_2, which is natural given the shorter bond lengths and smaller compressibility of the carbon compound.

It is interesting to rationalize the finding of edge-sharing tetrahedra in high-pressure CS_2, which behaves similarly to low-pressure SiS_2, whose phases consist of variously packed tetrahedra. The stability of phases with edge-sharing tetrahedra

TABLE I. Structural data of the new phases. As seen from the Wyckoff (Wyck.) positions, the number of CS_2 formula units per cell is $Z = 4$ for all the phases except HP2, where $Z = 12$.

$P = 50$ GPa

HP1 ($P2_1/c$)

			x	y	z	Wyck.
Coordinate	C		0.153	−0.355	−0.322	4e
	S		0.277	−0.091	−0.435	4e
	S		0.235	0.126	0.023	4e
Lattice		a	b	c	β	Volume
		4.86	5.59	4.74	110.02	120.95

$P = 20$ GPa

HP2 ($P2_1/c$)

			x	y	z	Wyck.
Coordinate	C		0.355	−0.133	−0.499	4e
	C		0.213	−0.365	−0.332	4e
	C		−0.061	0.362	−0.336	4e
	S		−0.438	−0.105	0.412	4e
	S		0.067	−0.131	0.423	4e
	S		0.415	−0.374	−0.419	4e
	S		0.275	−0.133	−0.243	4e
	S		−0.079	−0.388	−0.412	4e
	S		0.227	0.388	−0.251	4e
Lattice		a	b	c	β	Volume
		6.21	6.42	11.49	105.01	442.17

$P = 10$ GPa

NP ($Ibam$)

			x	y	z	Wyck.
Coordinate	C		0.000	0.000	0.250	4a
	S		0.122	−0.206	0.000	8j
Lattice		a	b	c	α,β,γ	Volume
		6.96	5.09	4.83	90	171.21

in a carbon compound such as CO_2 is denied by Pauling's third rule for ionic crystals, which states that edge sharing has a destabilizing effect because it brings the positive carbon ions too close together, increasing their Coulomb repulsion energy. The question is then why this obstacle does not arise in CS_2. In order to compare the importance of this effect on CO_2 and CS_2 we structurally optimized CO_2 in the HP1 structure at 50 GPa. In agreement with Pauling, we found for this structure a much higher enthalpy (by 0.4 eV/molecule) with respect to the stable phase β-cristobalite, showing that edge sharing in CO_2 is indeed unfavorable. To confirm that this is due to ionicity, we calculated Bader charges [25,26] for the C, S, and O atoms in the HP1 structure. Strikingly, whereas in CO_2 the partial charge of carbon is about $+2$, it turned out to be about -0.5 in CS_2. The bond polarization in CS_2 is not only of small magnitude but opposite to that in CO_2. This finding explains why edge sharing in CS_2 does not have the destabilizing effect it has in CO_2. A second significant difference between CO_2 and CS_2 originates from the different chemistries of oxygen and sulfur, which become relevant at higher pressures where the chalcogen binds two carbons. In this configuration, oxygen hybridizes sp^3, favoring a bond angle of about 109°; sulfur instead prefers p orbital binding without hybridization and a bond angle closer to 90°. (See a detailed discussion in, e.g., Ref. [27]). Therefore, it is not surprising to find that CO_2 adopts the β-cristobalite structure where the C-O-C bond angles are 106° and 115°, while CS_2 prefers the edge-sharing tetrahedra with a C-S-C bond angle of 90°.

Figure 3 shows the calculated diffraction pattern of the HP1 and β-cristobalite structures of CS_2 at 50 GPa. Comparing
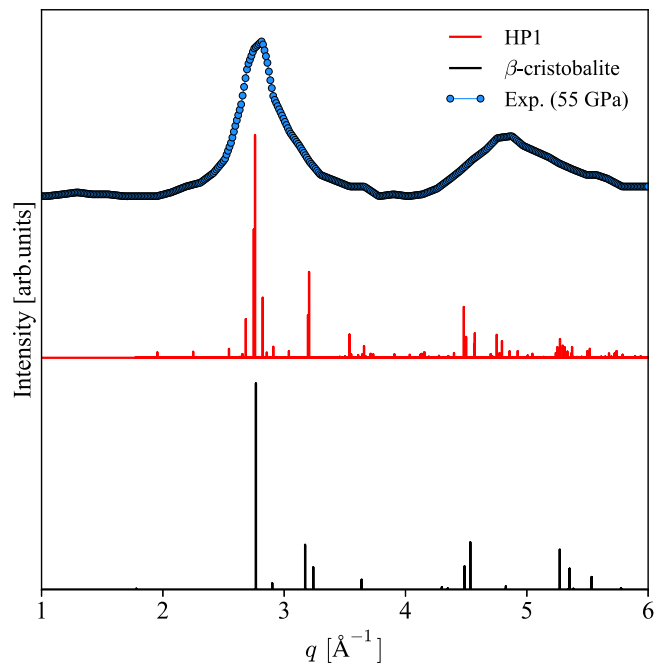

FIG. 3. (Color online) Calculated x-ray diffraction patterns of the HP1 and β-cristobalite structures of CS_2 at $P = 55$ GPa, compared with experimental data from Ref. [7]
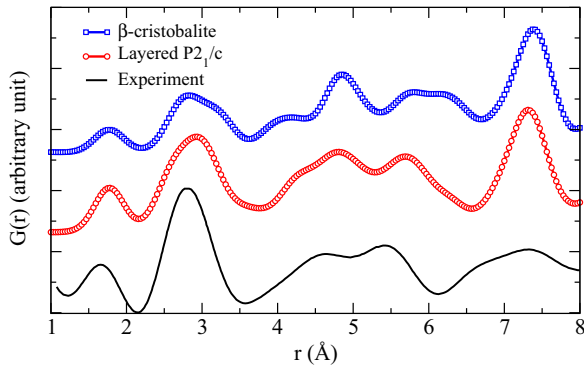
FIG. 4. (Color online) Calculated pair correlations $G(r)$ at 50 GPa for β-cristobalite (blue) and layered HP1 (red) in comparison with experimental data at 55 GPa taken from Ref. [9]. An empirical Gaussian broadening was applied to $G(r)$ of the respective perfect crystals in order to mimic the structural disorder. The Gaussian width was chosen in order to get for the C-S bond peak at 1.75 Å the same width as in experiment [7].

the positions of the Bragg peaks with those of the broad peaks of the x-ray structure factor $S(Q)$ in experiment at 55 GPa (Fig. 3 in Ref. [7]), we find roughly the same agreement for both crystalline structures. In order to discuss and compare more realistically the direct-space pair correlation function, we carried out an *ab initio* molecular dynamics simulation for HP1-CS$_2$ and β-cristobalite CS$_2$ at 300 K and $P = 0$ GPa, using the VASP code. Figure 4 shows the results in comparison with the experimentally extracted $G(r)$ [7]. Although differences are not dramatic, the HP1 pair correlations appear to agree with experiment somewhat better than those for β-cristobalite. As a side result, these simulations also indicated a high level of stability and robustness of HP1-CS$_2$ against thermal fluctuations. It is believed that this stability will be important for later tribochemical studies which we are planning.

IV. PHONONS, RAMAN, AND INFRARED ABSORPTION SPECTRA

In order to ascertain mechanical and dynamical stability and in preparation for spectroscopy, we calculated the phonon spectrum of the main HP1 phase that dominates the phase diagram of CS$_2$ for a wide range of pressures. As shown in Fig. 5, at $P = 50$ GPa all mode frequencies are real and positive, confirming the mechanical stability of the structure. Comparison with calculated phonons of the β-cristobalite structure [7] shows that modes of the HP1 layered structure are slightly stiffer, although there is a fair amount of overall similarity. Phonon calculations for HP2, which are prohibitively expensive because of the large 36-atom unit cell, were not attempted, given the uncertain stability of this phase.

Based on these phonon calculations, we subsequently calculated the Raman and IR absorption spectra of the HP1 structure and compared them with β-cristobalite. These spectral calculations require an insulating electronic structure. Therefore, even if available data were mostly at higher pressures, we conducted our spectral calculations at 20 GPa,
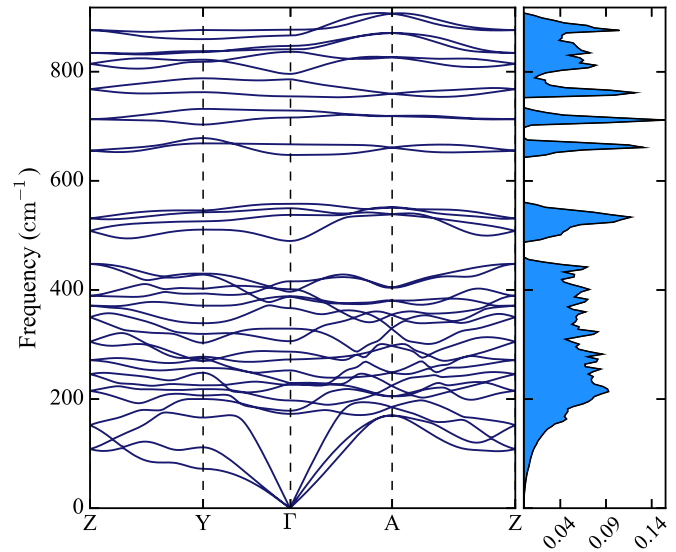

FIG. 5. (Color online) Calculated phonon spectrum of the HP1 layered structure of CS$_2$ at 50 GPa.

where both HP1 and β-cristobalite still have insulating LDA band structures. Actually, we found that LDA at 20 GPa yielded a similar volume to that of GGA at 30 GPa and that the crystal structures underlying these LDA spectral calculations are not very different from those of our previous 50-GPa structural determinations. As shown in Fig. 6, the differences between the layered HP1 and β-cristobalite predicted spectra are major. The Raman spectrum of β-cristobalite has a main (twin) peak near 300 cm^{-1}, a second main peak near 400 cm^{-1}, much weaker features near 600–700 cm^{-1}, and nothing at higher frequencies. The HP1 Raman predicted spectrum exhibits instead a much larger peak near 500 cm^{-1} and considerable spectral intensity at 700 and 800 cm^{-1}. Both the 500 and the 800 features agree much better with experimental Raman data
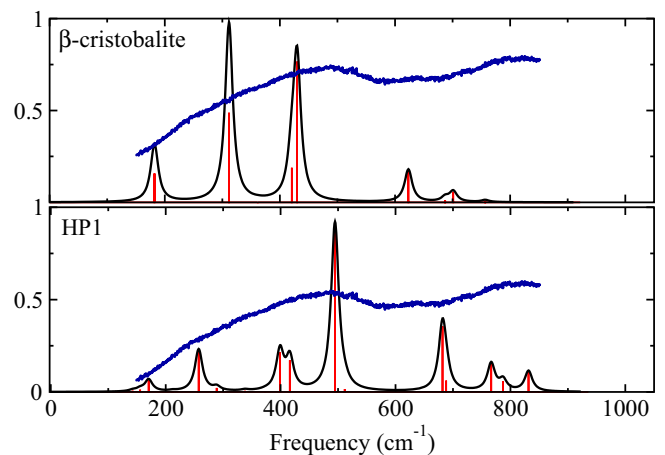

FIG. 6. (Color online) Predicted Raman spectra of two competing CS$_2$ structures at 50 GPa, compared with measurements at 50 GPa, 297 K [7]. The high-frequency secondary peak near 800 cm^{-1} is only present in layered HP1 and is absent in β-cristobalite. Also the low-frequency spectrum is better reproduced by HP1 than by β-cristobalite.
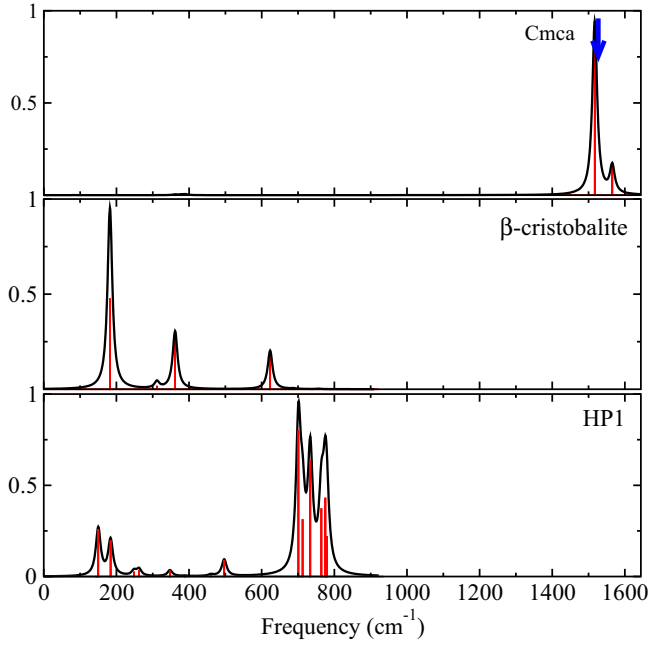
FIG. 7. (Color online) Calculated IR spectra of different CS_2 structures. Note the stiffer frequencies of layered HP1 compared with β-cristobalite. Blue arrows indicate the experimental IR peak positions of molecular CS_2 [28,29].

(50 GPa, 297 K) [7]. This proves that HP1 is more likely to be the dominant phase of CS_2, as opposed to β-cristobalite, near 50 GPa.

Besides Raman spectra, high-pressure systems should also permit the measurement of IR absorption. We therefore calculated IR spectra, which not surprisingly turned out to be very different for the layered HP1 and for β-cristobalite. As can be observed in Fig. 7, the main predicted absorption peaks of β-cristobalite are close to $\approx$200, 350, and 610 cm^{-1}. In the HP1 phase, after a weaker structure between 150 and 200 cm^{-1}, there is instead a large and broad absorption band between 700 and 800 cm^{-1}, a range where β-cristobalite should be IR silent. In future data, this unmistakable difference of IR absorption spectra should stand out clearly. Experimental IR data exist apparently only for the low-pressure molecular structure. The IR peak positions observed for the *Cmca* structure represented by the arrow in Fig. 7 agree very well with our calculations.

V. ELECTRONIC STRUCTURE

DFT calculations yield the electron band structure of all low-enthalpy phases of CS_2. All low-pressure structures are insulating. The DFT-PBE electronic band structure of the layered HP1 phase is shown in Fig. 8(b) at 40 GPa, above the critical metallization pressure, where the band gap of HP1-CS_2 closes. Metallization of HP1-CS_2 occurs at about 30 GPa within the PBE functional, an approximation which notoriously underestimates the gap and therefore the metallization pressure. We repeated the CS_2 calculations using the Becke, three-parameter, Lee-Yang-Parr hybrid functional (B3LYP) [32] and found that the metallization pressure increases to
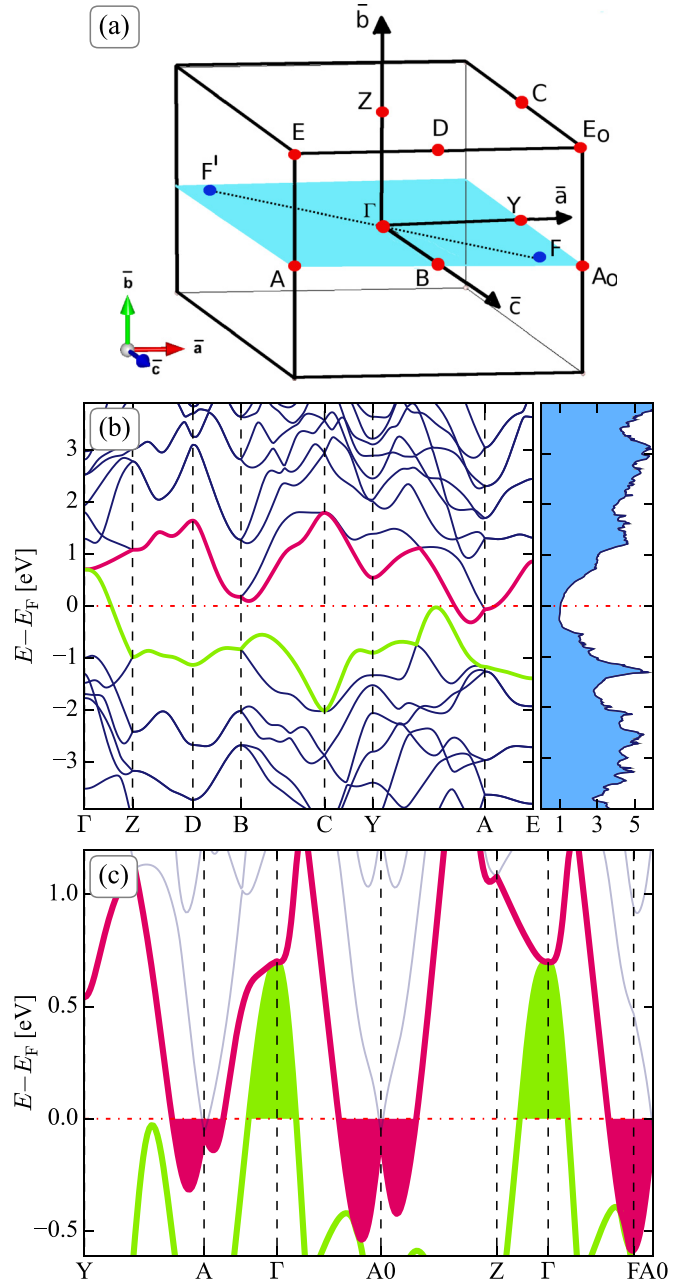

FIG. 8. (Color online) (a) The parallelepiped Brillouin zone of the HP1 $P2_1/c$ structure [30,31]. $F = (0.3636, 0.0000, 0.4545)$ is a general point in the Brillouin zone. (b) PBE electronic structure of HP1-CS_2 at 40 GPa, above the insulator-metal transition. (c) Bands near the Fermi level showing a single hole pocket at Γ and two electron pockets at F and $F' = -F$.

$\approx$50 GPa, a value now in excellent agreement with experiment [7]. It is interesting to note that, owing to its band gap initially being smaller than that of CO_2, CS_2 metallizes readily under pressure after changing from a twofold molecular state to a dense fourfold solid, unlike CO_2, which remains a wide-gap insulator long after a similar transformation into β-cristobalite. One interesting question arising at this point is whether superconductivity is predicted in the metallic high-pressure state of HP1-CS_2. Unfortunately, our limited resources and

the large 12-atom unit cell prevented us from calculating the electron-phonon interaction λ and thus estimating the critical temperature T_c. Nonetheless, a qualitative answer to that question, even before any detailed calculations are carried out, is suggested by direct inspection of the band structure of Fig. 8(c). Metallization of HP1 takes place via band overlap, with formation of a hole pocket at the $k = 0$ Γ point and a corresponding pair of electron pockets at k points F and F' near A_0 and A but off the Γ-A_0 line. The electron density of states of Fig. 8(c) calculated after band overlap is small, not suggestive of a large electron-phonon coupling parameter λ. As in other cases, our observation of band overlap metallization [33] does not offer a strong promise of superconductivity, at least of the standard BCS kind. However, the wave vectors Γ-F and Γ-F', with $F, F' = \pm(0.3636, 0.0000, 0.4545)$, are electron-hole nesting vectors of HP1-CS_2 near the gap-closing pressure around 50 GPa. It is possible that charge-density-wave or spin-density-wave static modulations might appear with that periodicity, possibly also accompanied by some related superconducting phase. We are not presently in a position to inquire quantitatively into this possibility, which would require newer and different approaches.

VI. CONCLUSIONS

We presented a theoretical study of high-pressure solid phases of CS_2. We discarded the obvious possibility of decomposition by restricting ourselves to only phases devoid of C-C and of S-S nearest-neighbor bonds and aiming at uncovering the metastable phases of lowest enthalpy through an unbiased evolutionary structure search. Our main result is that, contrary to expectations based on the similarity of CS_2 to CO_2, where twofold coordinated $Cmca$ eventually turns into fourfold coordinated β-cristobalite, high pressure in CS_2 eventually converts $Cmca$ into a different fourfold coordinated layered $P2_1/c$ phase made up of edge-sharing pairs of tetrahedra. Recently, the very same structure, named HP1, was experimentally reported for SiS_2 at much lower pressures [10]. Another tetrahedra-based structure, HP2, is also stabilized between 8 and 30 GPa, but only by a small enthalpy difference with respect to HP1 that is comparable to our calculation errors.

The proposed HP1 structure represents a more plausible candidate structure for high-pressure, fourfold coordinated CS_2 than those considered so far [7,9]. Both calculated pair correlations and Raman spectra agree better with existing data than those of β-cristobalite. It will be a challenge for experimentalists to try to prepare this phase in a crystalline state amenable to more accurate investigation in the future. To that end we provide substantial additional predictions, in particular of IR spectra, that should be crucial in identifying the new phase. Despite its intrinsic metastability, the HP1-CS_2 structure appears to be exceptionally robust. These qualities make CS_2 a good candidate system for studies of high-pressure simulated tribochemistry, a project which is presently going on in the Trieste group.

Even though the layered HP1 structure is metallic above 50 GPa, it seems unlikely that it should account for the experimentally observed superconductivity [9] because the density of states, and therefore the dimensionless λ,

is likely to remain low after the band-overlap metallic state. Although a reasonable hypothesis could be a possible partial decomposition of CS_2, with the creation of some free-sulfur filaments or other nonstoichiometric products, we are not in a position to address that occurrence here.

We note in closing that at pressures just before metallization, where the band gap closing of insulating HP1-CS_2 is indirect, the crystal might develop a narrow charge-density-wave or spin-density-wave phase, characterized by a nesting wave vector close to $\pm F$ [34]. Although there has been so far no observation of this kind in high-pressure experiments, this possibility, which we also suggested for MoS_2 [35], seems worth pursuing.

Last, and perhaps most important, our work provides a link to the high-pressure crystal chemistry of the archetypal family of IV–VI AB_2 compounds made of light elements for which only some cross similarities between CO_2, SiO_2, and SiS_2 were previously discussed. We show that there is some structural kinship of CS_2 not just to CO_2 at low pressures but eventually also to SiS_2 at higher pressures.

Note added. Recently, we became aware of work by Zarifi *et al.* [36], who theoretically investigated possible high-pressure metastable phases of CS_2 using a crystal-structure search without constraints, thus allowing for C-C and S-S bonds. Their approach is based on the assumption that kinetics could prevent complete decomposition but could not prevent access to such metastable phases. That work is actually ideally complementary to ours. At 55 GPa, our HP1 phase has, of course, a higher enthalpy than their $P2_1/m$ phase, where C-C and S-S bonds appear and whose enthalpy is, in turn, still much higher than full decomposition into carbon and sulfur. Before imposing our constraint, we too had found several lower-enthalpy phases with C-C and S-S bonds, but they carried a level of arbitrariness connected to the choice of cell size that made them hard to trust. Our work, on the other hand, takes the viewpoint that slow kinetics would be so dominant at high pressures and low temperatures that it would not only impede decomposition but also suppress atom migrations necessary to form any sort of C-C and S-S first-neighbor bonds. It should also be noted that the experimental data show no diffraction evidence at 55 GPa of either C-C bonds with a length around 1.5 Å or S-S bonds with a length around 2.2 Å, suggesting that such metastable phases might not be easily attained kinetically. Future IR measurements or another discriminating experiment should be able to compare the two different suggestions. We are grateful to J. Tse for correspondence and information on this matter.

---

[1] V. Iota, C. S. Yoo, and H. Cynn, Science **283**, 1510 (1999).

[2] S. Serra, C. Cavazzoni, G. L. Chiarotti, S. Scandolo, and E. Tosatti, Science **284**, 788 (1999).

[3] M. Santoro, F. A. Gorelli, R. Bini, J. Haines, O. Cambon, C. Levelut, J. A. Montoya, and S. Scandolo, Proc. Natl. Acad. Sci. USA **109**, 5176 (2012).

[4] J. Sun, D. D. Klug, R. Martoň;ák, J. A. Montoya, M.-S. Lee, S. Scandolo, and E. Tosatti, Proc. Natl. Acad. Sci. USA **106**, 6077 (2009).

[5] J. D. Cox, D. D. Wagman, and V. A. Medvedev, *CODATA Key Values for Thermodynamics* (Hemisphere, New York, 1984).

[6] M. J. Chase, J. Phys. Chem. Ref. Data Monogr. **9**, 1 (1998).

[7] R. P. Dias, C.-S. Yoo, M. Kim, and J. S. Tse, Phys. Rev. B **84**, 144104 (2011).

[8] F. Bolduan, H. D. Hochheimer, and H. J. Jodl, J. Chem. Phys. **84**, 6997 (1986).

[9] R. P. Dias, C.-S. Yoo, V. V. Struzhkin, M. Kim, T. Muramatsu, T. Matsuoka, Y. Ohishi, and S. Sinogeikin, Proc. Natl. Acad. Sci. USA **110**, 11720 (2013).

[10] J. Evers, P. Mayer, L. Möckl, G. Oehlinger, R. Köppe, and H. Schnöckel, Inorg. Chem. **54**, 1240 (2015).

[11] C. W. Glass, A. R. Oganov, and N. Hansen, Comput. Phys. Commun. **175**, 713 (2006).

[12] A. R. Oganov and C. W. Glass, J. Chem. Phys. **124**, 244704 (2006).

[13] A. O. Lyakhov, A. R. Oganov, H. T. Stokes, and Q. Zhu, Comput. Phys. Commun. **184**, 1172 (2013).

[14] A. R. Oganov, A. O. Lyakhov, and M. Valle, Acc. Chem. Res. **44**, 227 (2011).

[15] Q. Zhu, A. R. Oganov, C. W. Glass, and H. T. Stokes, Acta Crystallogr., Sect. B **68**, 215 (2012).

[16] J. P. Perdew, K. Burke, and M. Ernzerhof, Phys. Rev. Lett. **78**, 1396 (1997).

[17] G. Kresse and J. Furthmüller, Phys. Rev. B **54**, 11169 (1996).

[18] P. E. Blöchl, Phys. Rev. B **50**, 17953 (1994).

[19] G. Kresse and D. Joubert, Phys. Rev. B **59**, 1758 (1999).

[20] J. Klimeš, D. R. Bowler, and A. Michaelides, J. Phys. Condens. Matter **22**, 022201 (2010).

[21] J. Klimeš, D. R. Bowler, and A. Michaelides, Phys. Rev. B **83**, 195131 (2011).

[22] M. Dion, H. Rydberg, E. Schröder, D. C. Langreth, and B. I. Lundqvist, Phys. Rev. Lett. **92**, 246401 (2004).

[23] P. Giannozzi *et al.*, J. Phys. Condens. Matter **21**, 395502 (2009).

[24] T. A. Guseva, K. P. Burdina, K. N. Semenenko, and K. P. Semenenko, Mask. Gos. Univ.. Ser. 2: Khimiya **32**, 85 (1991).

[25] R. F. W. Bader, *Atoms in Molecules: A Quantum Theory* (Oxford University Press, New York, 1990).

[26] G. Henkelman, A. Arnaldsson, and H. Jónsson, Comput. Mater. Sci **36**, 354 (2006).

[27] J. E. House, *Inorganic Chemistry* (Elsevier, Amsterdam, 2008).

[28] S. F. Agnew, R. E. Mischke, and B. I. Swanson, J. Phys. Chem. **92**, 4201 (1988).

[29] H. Yamada and W. B. Person, J. Chem. Phys. **40**, 309 (1963).

[30] M. I. Aroyo, J. M. Perez-Mato, C. Capillas, E. Kroumova, S. Ivantchev, G. Madariaga, A. Kirov, and H. Wondratschek, Z. Kristallogr. **221**, 15 (2006).

[31] M. I. Aroyo, A. Kirov, C. Capillas, J. M. Perez-Mato, and H. Wondratschek, Acta Crystallogr., Sect. A **62**, 115 (2006).

[32] A. D. Becke, J. Chem. Phys. **98**, 5648 (1993).

[33] O. Kohulák, R. Martoňák, and E. Tosatti, Phys. Rev. B **91**, 144113 (2015).

[34] D. Jérome, T. M. Rice, and W. Kohn, Phys. Rev. **158**, 462 (1967).

[35] L. Hromadová, R. Martoňák, and E. Tosatti, Phys. Rev. B **87**, 144105 (2013).

[36] N. Zarifi, H. Liu, and J. S. Tse, Sci. Rep. **5**, 10458 (2015).